Molecular Cancer Research

COP35, a Cholangiocarcinoma-Binding Oligopeptide, Interacts with the Clathrin Heavy Chain Accompanied by GRP78

Hiroe Kitahara, Junya Masumoto, Alan L. Parker, et al.

Mol Cancer Res 2011;9:688-701. Published OnlineFirst May 13, 2011.

Published OnlineFirst May 13, 2011; DOI:10.1158/1541-7786.MCR-10-0470

Angiogenesis, Metastasis, and the Cellular Microenvironment

Molecular Cancer Research

COP35, a Cholangiocarcinoma-Binding Oligopeptide, Interacts with the Clathrin Heavy Chain Accompanied by GRP78

Hiroe Kitahara[1], Junya Masumoto[2], Alan L. Parker[3], Fukuto Maruta[1], Naoki Kubo[1], Akira Shimizu[1], Noriyuki Akita[1], Shiro Miwa[1], Naoya Kobayashi[4], Jun Nakayama[2], and Shinichi Miyagawa[1]

Abstract

Cholangiocarcinoma (CCA) is a common carcinoma of the liver, and the majority of patients with CCA have a poor prognosis due to the lack of effective nonsurgical therapies in addition to its rapid progression and inoperability at the time of diagnosis. The development of novel nonsurgical therapeutics that efficiently target CCA could significantly improve the prognosis for patients presenting with CCA. Here, we describe the iterative production and characterization of a novel peptide, designated COP35 (CCA-binding oligopeptide 35), which binds selectively to human CCA, identified by bacteriophage biopanning using the intrahepatic CCA cell line RBE and the normal cholangiocyte cell line MMNK-1. COP35 was found to augment the growth inhibitory effects of 5-fluorouracil (5-FU) against RBE cells. Utilizing pull-down assay and liquid chromatography, we identify the clathrin heavy chain accompanied by GRP78/BiP as a COP35-binding partner. In summary, we identify COP35 as a possible candidate for peptide-targeted therapies for CCA. *Mol Cancer Res; 9(6); 688–701.* ©*2011 AACR.*

Introduction

Cholangiocarcinoma (CCA) is a highly malignant tumor that arises from the ductal epithelium of the biliary tree and is a common secondary carcinoma of the liver (1). The incidence and mortality rates of CCA are increasing worldwide (2). Although tumors originating from the common hepatic or bile duct are readily identifiable owing to obstructive jaundice, tumors originating from the small bile duct do not cause significant biliary obstruction until the tumor itself or metastatic lesions cause obstruction of the common hepatic or bile duct (3). In terms of treatment, complete surgical resection remains the only effective means to cure patients with CCA owing to the difficulty of early diagnosis and the rapid progression of the disease. The main obstacles to complete resection for CCA are the multiplicity of the lesions, that is, multicentric occurrence, intrahepatic extension, and distant metastasis. Therefore, establishment of a methodology that could efficiently target CCA could dramatically improve the efficacy of treatments for CCA. Most patients with unresectable disease at clinical presentation have a poor prognosis (5-year survival rates are 0%–40% even in resected cases; refs. 2, 4). Furthermore, CCA responds poorly to chemotherapy, and radiation therapy and conventional treatments are not adequate for the vast majority of patients with CCA. Moreover, conventional chemotherapy and radiation therapy have shown no efficacy in extending median survival rates, and although photodynamic therapy combined with stenting has been reported to be effective as a palliative treatment, it is not curative. Thus, the development of novel chemopreventive and adjuvant therapeutic strategies based on exploring select molecular targets could impact significantly upon clinical outcomes.

The studies of several groups have identified potential candidate molecular targeting agents to achieve tumor tropism. The ligands that have been evaluated include antibodies, single-chain fragment variables, and growth factors (5–7). More recently, peptide-presenting bacteriophage libraries that enable the selection of peptides that bind to selected cell types or ligands have been utilized (8). The biopanning technique has been shown to be a powerful tool for identifying specific ligands on target organs and tumors, as it enables forced evolution of very high-affinity targeting peptides through rounds of selection of living libraries of peptides presented on the surface of the bacteriophage particle (9–12). This technique has classically been used to iteratively produce peptides binding purified cell surface markers (13, 14), cultured cell lines (15, 16), or tumor-bearing animals (17–19). We utilized a peptide-presenting bacteriophage library on the basis of a combinatorial library of random

Authors' Affiliations: Departments of [1]Surgery and [2]Pathology, Shinshu University School of Medicine, Nagano, Japan; [3]BHF Glasgow Cardiovascular Research Centre, University of Glasgow, Glasgow, Scotland, United Kingdom; and [4]Department of Surgery, Okayama University Graduate School of Medicine and Dentistry, Okayama, Japan

Corresponding Author: Junya Masumoto, Department of Pathology, Shinshu University School of Medicine, Asahi 3-1-1, Matsumoto 390-8621, Nagano, Japan. Phone: 81-263-37-3395; Fax: 81-263-37-2581. E-mail: masumoto@shinshu-u.ac.jp or Shinichi Miyagawa, Department of Surgery, Shinshu University School of Medicine, Asahi 3-1-1, Matsumoto 390-8621, Nagano, Japan. Phone: 81-263-37-2654; Fax: 81-263-35-1282; E-mail: shinichi@shinshu-u.ac.jp

doi: 10.1158/1541-7786.MCR-10-0470

Published OnlineFirst May 13, 2011; DOI:10.1158/1541-7786.MCR-10-0470

peptide 12mers fused to a minor coat protein pIII of the M13 bacteriophage containing approximately 2.7×10^9 different sequences, and different peptides selective for the target cells were identified with successive rounds of biopanning. We identified a new oligopeptide (designated COP35) that specifically bound to CCA cells and its target molecules. We characterized the effects of the selected peptide on tumor inhibition in combination with anticancer agents and elucidated a potential binding partner for COP35.

Materials and Methods

Patient materials

Frozen and paraffin-embedded sections of human liver and biliary duct tissue with or without tumors were obtained from Shinshu University Hospital. The analysis of patient materials was approved by the Human Research Ethical Committee of Shinshu University, School of Medicine. Written informed consent for resection was obtained from the patients.

Cell lines

The human cholangiocyte cell line MMNK-1 was provided by the Department of Surgery of Okayama University School of Medicine and was maintained as described previously (20, 21). The human intrahepatic cholangiocarcinoma (ICC) cell line RBE, human ICC cell line HuH-28, human ICC cell line IHGGK, human hepatocellular carcinoma cell line Hep3B, and human extrahepatic bile duct carcinoma (ECC) cell line TFK-1 were supplied by the Cell Resource Center for the Biomedical Research Institute of Development, Aging, and Cancer of Tohoku University (Sendai, Japan). HuH-28 cells were maintained in minimum essential medium (Invitrogen) containing 10% FBS supplemented with 100 units/mL penicillin and 100 mg/mL streptomycin at 37°C in 5% CO_2. All other cell lines were maintained in Dulbecco's modified Eagle's medium (DMEM; Invitrogen) containing 10% FBS supplemented with 100 units/mL penicillin and 100 mg/mL streptomycin at 37°C in 5% CO_2.

Phage display, isolation, and sequencing of phage DNA

The biopanning procedure was carried out as described previously (12). Briefly, we utilized the M13 phage display 12-peptide library constructed using Phage Display Peptide Library Kit (New England Biolabs). MMNK-1 cells were used as absorber cells for whole-cell subtractive screening, and RBE cells were used as the target cells. Biopanning was conducted for a total of 3 rounds for enrichment of peptides binding selectively and efficiently to CCA. Phage display, isolation, and sequencing of phage DNA were carried out as described previously (10, 11).

Peptide preparation

Custom peptides COP35 "TPVLETPKLLLW," a control peptide "HAKSPEMCTFVG," which has almost the same net hydrophobic/hydrophilic and charge properties as COP35, and trans-acting activator of transcription (TAT) peptide "GRKKRRQRRRPPQ" were purchased from SIGMA Lifescience Custom Peptide Service (SIGMA Genosys). Synthetic peptides were high-performance liquid chromatography (HPLC) purified (>95%) with N-terminal biotinylation or *N*-hydroxy-succinimidyl (NHS)-fluorescein conjugation.

Evaluation of phage clones for their ability to bind to human cancer cells

The evaluation of binding activity of selected phage clones to human cell lines was conducted as described previously (11). RBE cells were cultured and plated into 96-well plates (1×10^4 cells per well) the day before use. The cells were washed and fixed in 4% paraformaldehyde in PBS for 20 minutes. 1×10^{10} plaque-forming units (pfu) per well of each selected phage clone was added to the cells at 4°C, unbounded phage were removed by washing cells with PBS, and bound phage were detected by cell-based ELISA.

Fluorescence microscopy of living cells with synthesized NHS-fluorescein–labeled peptides

Cells were cultured overnight in 8-well chamber slides and were washed 3 times with PBS containing 10% FBS. The cells were then incubated with 1.7 mg/mL NHS-fluorescein–labeled peptide (Sigma Genosys) for 2 hours at 37°C. After 2 hours, the medium was discarded and the cells were washed again with PBS containing 10% FBS and then stained with medium containing 4′,6-diamidino-2-phenylindole (DAPI) for nuclear counterstaining (Invitrogen), and the samples were imaged using a fluorescence microscope.

Fluorescence microscopy of NHS-fluorescein–labeled peptides binding to human resected tissue and fixed RBE cells

Frozen sections from human resected tissues and RBE cells were stained with NHS-fluorescein–labeled COP35 or control peptide. Optimal cutting temperature (OCT) compound (Tissue-Tek; Sakura Finetek)-embedded frozen sections (10-μm thick) were incubated with 100 μmol/L NHS-fluorescein–labeled peptide (green) for 2 hours at room temperature. Sections were counterstained with DAPI for nuclear counterstaining (Invitrogen), and the sections were imaged using a fluorescence microscope. For triple staining of frozen sections, they were incubated with 100 μmol/L NHS-fluorescein–labeled peptide (green) and anti-CHC mouse monoclonal antibody with Alexa-Fluor 647–conjugated secondary antibody (blue; 1:500 dilution; Cell Signaling Technology), and anti-GRP78 rabbit polyclonal antibody with trimethylrhodamine (TMR)-conjugated secondary antibody (red; 1:20 dilution; DAKO) for 2 hours at room temperature and the sections were imaged using a fluorescence microscope. The RBE cells fixed in 4% paraformaldehyde and permeabilized with 100% methanol were incubated with anti-CHC mouse monoclonal antibody with fluorescein isothiocyanate (FITC)-conjugated secondary

Published OnlineFirst May 13, 2011; DOI:10.1158/1541-7786.MCR-10-0470

antibody (green; 1:40 dilution; DAKO) and anti-GRP78 rabbit polyclonal antibody with TMR-conjugated secondary antibody (red; 1:20 dilution; DAKO). The sample slides were imaged using a fluorescence microscope.

Evaluating the effect of clathrin depletion on COP35 cellular binding and uptake in living RBE cells

The clathrin-dependent endocytosis inhibitor, chlorpromazine hydrochloride, was purchased from Sigma-Aldrich. A total of 1×10^5 RBE cells/mL were incubated with 100 μmol/L NHS-fluorescein–labeled COP35 or a control peptide in the presence or absence of 5 μg/mL chlorpromazine hydrochloride for 2 hours. Then, green fluorescence signal was observed by fluorescence microscopy.

Evaluation of fluorescence intensity of COP35

For the COP35 binding to frozen sections, the fluorescence signal intensity of COP35 result of 3(+) is defined as strong complete submembranous signals and/or uniform intense intracellular signals; 2(+) is defined as weak complete submembranous signals and/or uniform intense intracellular signals; 1(+) is defined as weak, incomplete submembranous or partial intracellular signals in any proportion of tumor cells; and 0 is defined as there being no specific fluorescence signal.

Evaluation of cell growth

To gauge toxicologic side effects of the iteratively produced peptides, cell viability was evaluated by MTS assay. RBE cells were seeded in 96-well plates at 5×10^3 cells per well. The culture medium was replaced with 120 μL of medium containing 20 μL of CellTiter 96 AQueous One solution reagent (Promega), and the culture plates were incubated at 37°C for 2 hours. One hundred microliter of the medium was transferred to a new 96-well plate, and the quantity of the formazan product was determined by measuring the absorbance at 490 nm.

Peptide precipitation

RBE cells were lysed in 1 mL of NP-40 buffer [0.25% or 1% Nonidet P-40, 142.5 mmol/L KCl, 5 mmol/L $MgCl_2$, 10 mmol/L HEPES (pH 7.6), 0.2 mmol/L phenylmethylsulfonylfluoride (PMSF), and 1 mmol/L EDTA] with proteinase inhibitor cocktail Complete Mini (Roche-diagnostics; ref. 22). The lysate was mechanically dislodged from the plate. The lysate from 1 dish was incubated on ice, and centrifuged at 15,000 × *g* for 15 minutes. The supernatant was precipitated with 40 μL of streptavidin-conjugated agarose beads (Invitrogen) and 20 μL of diluted biotinylated peptide and incubated for 1 hour at 4°C. After incubation, the streptavidin-conjugated agarose beads were washed with lysis buffer 4 times and centrifuged for 1 minute, and the supernatant was discarded. The precipitated proteins were subjected to SDS-PAGE, and protein bands were excised from Coomassie brilliant blue–stained gel. The excised proteins were identified by liquid chromatography-mass spectrometry (nano LC-ESI-Q-TOF MS-MS) and then searched for in the National Center for Biotechnology Information (NCBI) nr protein database using their tandem mass spectra and the MASCOT algorithm (Matrix Science).

Immunoprecipitation

RBE cell lysate was prepared as peptide precipitation. The supernatant was precipitated with 40 μL of protein A–conjugated agarose beads (Invitrogen) and 20 μg of specific antibodies including anti-Myc rabbit polyclonal antibody (negative control for rabbit polyclonal antibody; sc-789; Santa Cruz Biotechnology), anti-GRP78 rabbit polyclonal antibody (positive control; ab21685; Abcam), anti-Flag mouse monoclonal antibody (negative control for mouse monoclonal antibody; M2; Sigma-Aldrich), or anti-CHC mouse monoclonal antibody (610499; BD) and incubated for 1 hour at 4°C. The precipitated proteins were subjected to SDS-PAGE and then immunoblotting as described previously (22).

Expression plasmids and siRNAs

CHC and GRP78 expression plasmids were cloned into the *Hin*dIII site of pcDNA3 (Invitrogen) by PCR using primer sets of GCAAGCTTGCCATGGCCCAGATTCTGCCAA and AGAAGCTTCACATGCTGTACCCAAAGCCAG, or into the *Kpn*I and *Xho*I sites of pcDNA3 by PCR using primer sets of ATGGTACCACCATGAAGCTCTCCCTGGTGG and ATCTCGAGCTACAACTCATCTTTTTCTGCT from human expressed sequence tag (EST) clones (Clone ID: 6045540 and 10004803, respectively) purchased from Openbiosystems. The plasmids were sequenced to ensure that the correct sequences were inserted. CHC- and GRP78-specific Trilencer-27 siRNA kits were purchased from OriGene Technologies.

Transfection of expression plasmids or siRNAs

A total of 1×10^4 RBE cells per 100 μL well were transfected with 0.34 μg of CHC and/or GRP78 expression plasmids or empty plasmid alone (negative control) by Lipofectamine 2000 (Invitrogen) in accordance with the manufacturer's instructions. A total of 1×10^4 RBE cells per 100 μL well were transfected with 1.67 pmol of CHC- and/or GRP78-specific siRNAs or universal scrambled negative control (USNC) siRNA by Lipofectamine 2000 in accordance with manufacturer's instructions.

Immunohistochemistry

Immunohistochemistry was carried out as described previously (11). Anti-CHC rabbit polyclonal antibody (ab24578; Abcam) or anti-GRP78 rabbit polyclonal antibody (ab21685; Abcam) was diluted 1:100 in blocking buffer and exposed to the tissues overnight at 4°C.

Evaluation of immunoreactivity of CHC and GRP78

For the protein expression in human sections, evaluation of immunoreactivity of anti-CHC and anti-GRP78 antibodies was as follows: 3(+) is defined as strong complete

Published OnlineFirst May 13, 2011; DOI:10.1158/1541-7786.MCR-10-0470

submembranous and uniform intense intracellular staining, 2(+) is defined as weak complete submembranous staining or uniform intense intracellular staining, 1(+) is defined as weak, incomplete submembranous or partial intracellular staining in any proportion of tumor cells, and 0 is defined as there being no specific staining.

Statistics

Results are presented as the mean and SD. Levels of significance were evaluated using Student's *t* test. A value of $P < 0.05$ was considered statistically significant. Correlation was measured using Pearson's product–moment correlation coefficient.

Results

Identification of peptide motifs binding to human CCA RBE cells

In vitro biopanning was carried out as described previously with slight modifications (10–12). Briefly, following subtractive clearance of the library using the normal cell line MMNK-1, 3 consecutive rounds of *in vitro* biopanning were carried out on the target human ICC RBE cells. After removal of unbound phage, the cell-associated phage were recovered from each round of biopanning by lysing the cells and pooled as candidate phage clones. Approximately, 1×10^{11} clones were screened through this iterative biopanning procedure. Finally, 40 clones were selected and their affinity was evaluated by cell-based ELISA (Fig. 1A). We selected a single phage clone, 35, expressing the sequence "TPVLETPKLLLW," which exhibited higher affinity to RBE cells than the other clones at the concentrations tested (Fig. 1A, #35). We defined the peptide as CCA-binding oligopeptide #35 (COP35).

Binding of COP35 to human CCA cell lines

To evaluate the affinity and specificity of COP35 to several cancer cell lines, binding assays were conducted in a variety of cell lines including ICC cell lines RBE, IHGGK, and HuH-28, the ECC cell line TFK-1, the hepatocellular carcinoma cell line Hep3B, and the normal cholangiocyte cell line MMNK-1. COP35 showed significantly higher affinity to cancerous cell lines, RBE, HuH-28, TFK-1, IHGGK, and Hep3B, than to normal cholangiocyte cell line MMNK-1 (Fig. 1B).

Fluorescence microscopy analysis of COP35 binding to RBE cells

To confirm the binding and specificity of COP35 to CCA cell lines, we utilized NHS-fluorescein–labeled COP35 for fluorescence microscopy. Fluorescence signal was observed in the ICC cell line RBE cells incubated with COP35 (Fig. 2A, top left), whereas no significant fluorescence was observed in the cholangiocyte cell line MMNK-1 cells incubated with COP35 (Fig. 2A, bottom left). Furthermore, no significant fluorescence was observed in RBE or MMNK-1 cells when a control peptide "HAKSPEMCTFVG," which retains the overall net hydrophobic/hydrophilic and charge properties, was used as a negative control (Fig. 2A, top and bottom middle). Fluorescence was observed in both RBE and MMNK-1 cells incubated with TAT peptide "GRKKRRQRRRPPQ" as a cell-penetrating positive control peptide (Fig. 2A, top and bottom right; ref. 23).

Evaluation of COP35 binding to clinically resected CCA samples

To test whether COP35 retained its capacity to bind to cells from samples from primary isolated CCA samples, 18 CCA cases and nontumorous liver and biliary tissues of

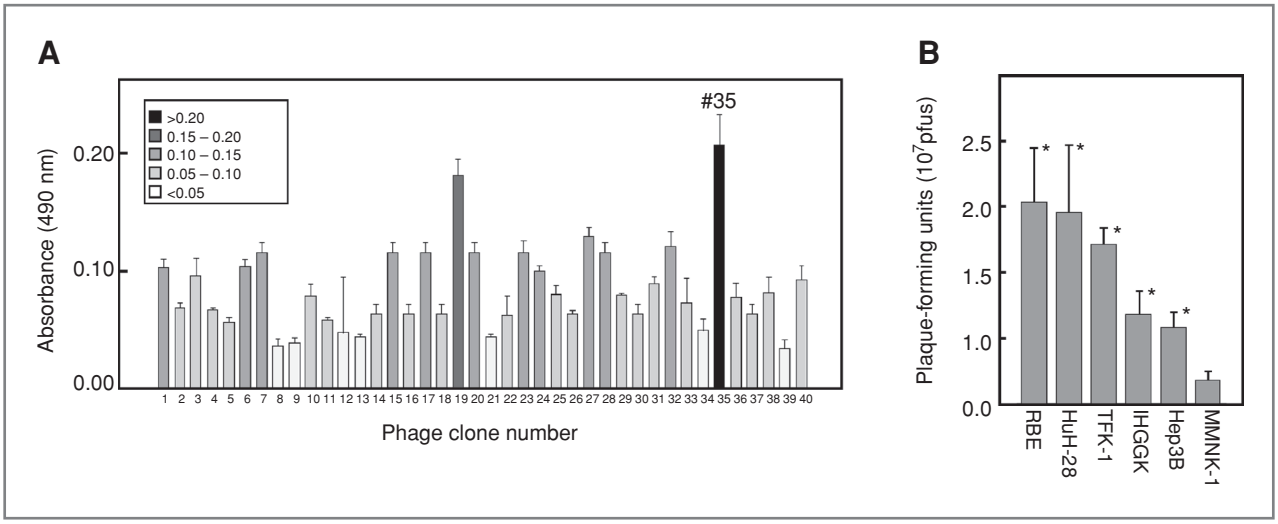

Figure 1. Evaluation of selected phage specificity. A, the affinities of 40 candidate clones were evaluated by cell ELISA. Absorbance is indicated on the left. Values represent the mean and SD from triplicate cultures. Clone #35 was selected for further studies. B, the binding of clone #35 was assessed in a variety of cell lines including ICC cell lines RBE, IHGGK, and HuH-28, the ECC cell line TFK-1, the hepatocellular carcinoma cell line Hep3B, and the normal cholangiocyte cell line MMNK-1. Pfus are indicated on the left. Values are the mean and SD from triplicate culture plates. *, $P < 0.01$.

Published OnlineFirst May 13, 2011; DOI:10.1158/1541-7786.MCR-10-0470

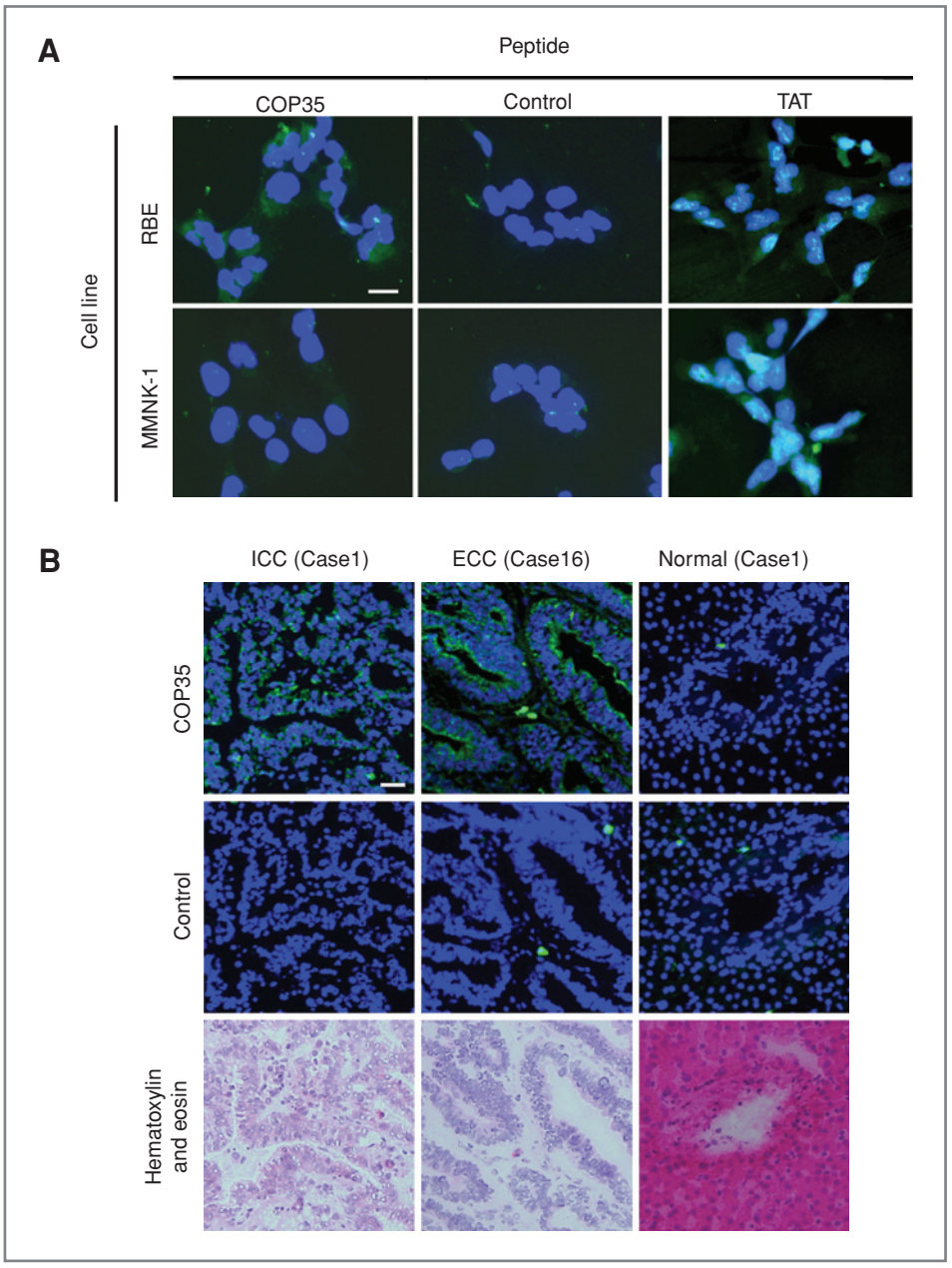

Figure 2. Fluorescence microscopy with NHS-fluorescein–labeled COP35 and MTS assay of RBE cells incubated with 5-FU and COP35. A, human CCA RBE cells (top) and human cholangiocyte MMNK-1 cells (bottom) were stained with NHS-fluorescein–labeled COP35 (left, COP35), a control peptide (middle, Control), or TAT peptide (right, TAT). A total of 100 μmol/L NHS-fluorescein–labeled peptides were incubated with RBE or MMNK-1 cells for 2 hours. Cell nuclei were counterstained with DAPI for nuclear counterstaining. Bar is 25 μm. B, fluorescence microscopy of frozen sections from CCA and nontumorous liver tissue with NHS-fluorescein–labeled COP35. The sections were incubated with 100 μmol/L NHS-fluorescein–labeled peptide for 2 hours at room temperature. Sections were counterstained with DAPI for nuclear counterstaining. Representative ICC (case 1 in Table 1), ECC (case 16 in Table 1), and nontumorous normal bile duct epithelium of CCA (case 1 in Table 1) are presented. Parallel hematoxylin and eosin staining images are shown (bottom). Bar is 100 μm.

the same samples were stained with the NHS-fluorescein–labeled COP35 peptide. The median age of the patients was 64.7 years (range: 34–77 years old), and 10 patients were male and 8 patients were female. The tumor histology is presented in Table 1. Representative figures are shown (Fig. 2B). Fluorescence was observed in the CCA samples including both ICC (Fig. 2B, left top, case 1) and ECC (Fig. 2B, middle top, case 16) with COP35, whereas no specific fluorescence was observed in these CCA tissues with the control peptide (Fig. 2B, left and middle middle, cases 1 and 16). Signals were hard to detect in nontumorous tissue sections in case 1 with either COP35 or the control peptide (Fig. 2B, right top and middle, case 1). Parallel hematoxylin and eosin staining images are presented (Fig. 2B, bottom).

Enhancement of the tumor inhibitory effect of 5-fluorouracil by COP35 against RBE cells

To evaluate whether COP35 could enhance the antitumor activity of 5-fluorouracil (5-FU) on RBE cells, tumor inhibitory effect was quantified in the presence of COP35 or control peptide (Fig. 2C). We next evaluated the effect on cell growth of 5-FU against RBE cells in the presence of COP35 or the control peptide by MTS assay (Fig. 2D). COP35 and 5-FU were added together and cell viability quantified after 36 or 48 hours of incubation.

Published OnlineFirst May 13, 2011; DOI:10.1158/1541-7786.MCR-10-0470

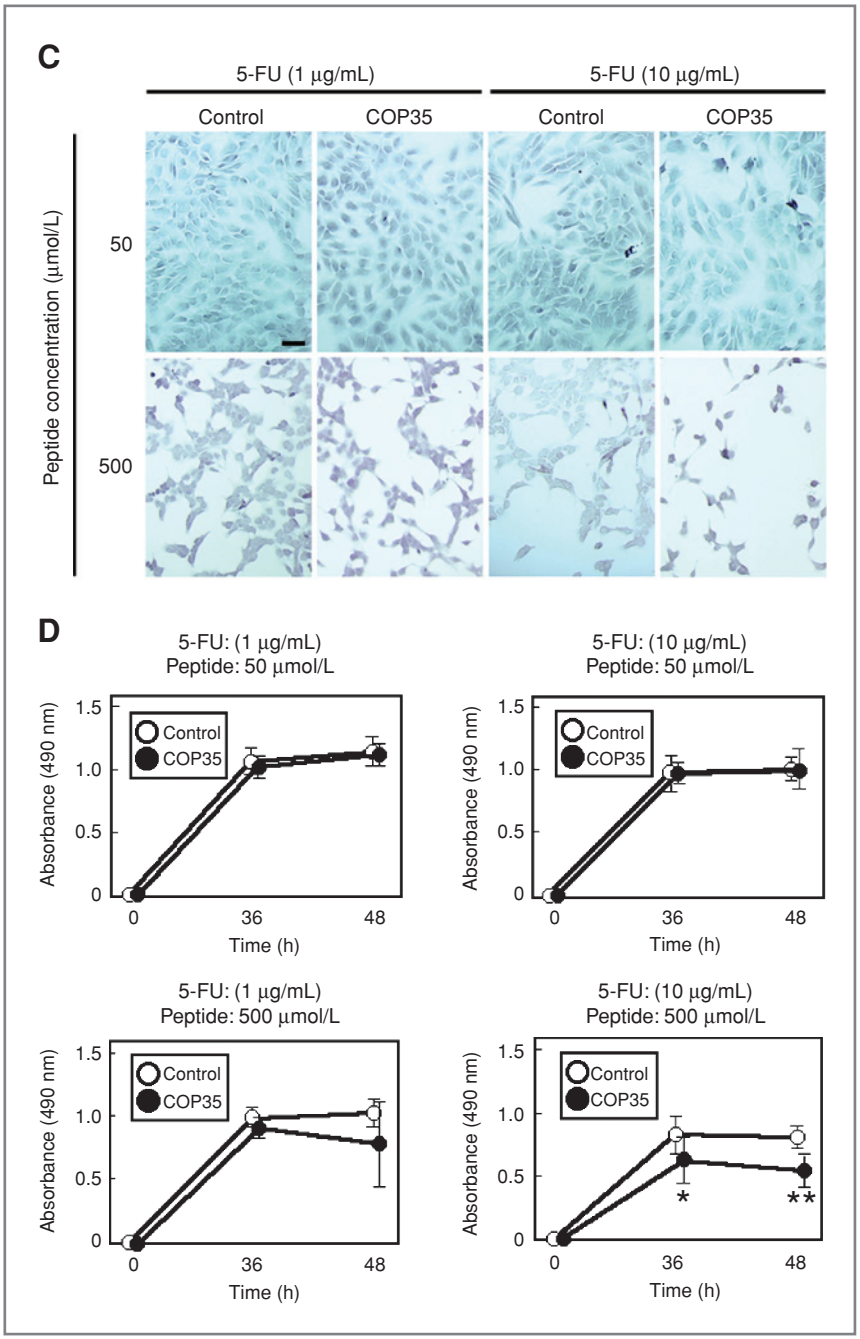

Figure 2. *(Continued)* C, tumor inhibitory effect of 5-FU with COP35 in RBE cells. RBE cells were incubated with 50 μmol/L (top) or 500 μmol/L (bottom) COP35 or control peptide with 1 μg/mL or 10 μg/mL 5-FU for 48 hours. The bar is 50 μm. D, MTS assay of RBE cells. RBE cells were plated in 96-well plates at 5×10^3 cells per well for 24 hours before the MTS assay. After 24 hours, cells were incubated with COP35 or the control peptide, and 1 μg/mL or 10 μg/mL 5-FU. After incubation for 36 and 48 hours, the growth inhibitory effect on the RBE cells was assessed. Values are the mean and SD results from triplicate cultures. *, $P < 0.05$; **, $P < 0.01$.

COP35 significantly enhanced the tumor inhibitory effect of 10 μg/mL 5-FU against RBE cells when it was incubated with 500 μmol/L COP35 following both 36 and 48 hours of incubation (Fig. 2D). The COP35 peptide alone showed no tumor inhibitory effect (Fig. 4A).

Identification of the COP35-binding partners

To identify putative binding partners for COP35, RBE cells were lysed with detergent concentrations of 0.25% or 1% NP-40 buffer and precipitated using biotinylated COP35 with streptavidin-conjugated agarose beads (Fig. 3A, left). As shown in the left panel of Figure 3A, a sharp band was found at approximately 190 kDa regardless of which buffer was used (Fig. 3A, left, arrowhead with band Q). Because the band lysed with 0.25% NP-40 buffer was clearer than that with 1.0% NP-40 buffer, we used 0.25% NP-40 buffer for the later analysis. In the peptide precipitation assay, as we decreased the concentration of COP35 in 0.25% NP-40 buffer, while we found only an approximately 190-kDa band precipitated with 20 μmol COP35 in lysis buffer (Fig. 3A, middle, arrowhead with band Q), another band was found

Published OnlineFirst May 13, 2011; DOI:10.1158/1541-7786.MCR-10-0470

Table 1. Clinicopathologic data, fluorescence signal intensity of COP35, and immunoreactivity of CHC and GRP78 in 18 CCA

Case	Age at surgery, y	Gender	Localization	Histology	COP35	CHC (T)	GRP78 (T)	CHC (NT)	GRP78 (NT)
1	62	M	I	wel-por	3+	3+	3+	1+	0
2	70	M	I	wel	3+	2+	3+	1+	0
3	55	M	I	wel-mod	3+	3+	1+	1+	0
4	67	M	I	por-mod	3+	3+	1+	2+	0
5	59	F	I	por	3+	3+	2+	2+	0
6	59	M	I	por-mod	2+	2+	1+	2+	0
7	77	M	I	wel	2+	3+	1+	1+	0
8	70	F	I	por	2+	3+	2+	1+	0
9	75	F	I	wel	2+	3+	1+	2+	1+
10	55	F	I	wel	2+	3+	1+	1+	0
11	67	F	I	wel	2+	2+	1+	1+	0
12	60	F	I	wel-mod	1+	1+	1+	0	0
13	68	M	I	mod-por	0	0	0	0	0
14	68	F	E	pap	3+	3+	1+	0	0
15	76	M	E	tub	3+	2+	1+	0	0
16	34	M	E	tub	3+	2+	1+	2+	0
17	72	F	E	tub	2+	2+	1+	–[a]	–
18	71	M	E	pap-tub	2+	2+	1+	–	–

Abbreviations: F, female; M, male; I, intrahepatic; E, extrahepatic; wel, well-differentiated adenocarcinoma; mod, moderately differentiated adenocarcinoma, por, poorly differentiated adenocarcinoma; tub, tubular adenocarcinoma; pap, papillary adenocarcinoma; T, tumorous tissue, N, nontumorous tissue.

[a]There is no nontumorous tissue.

to appear around 80 kDa precipitated with 4.0 and 2.0 μmol COP35 in lysis buffer (Fig. 3A, middle, arrowhead with band R). The band disappeared at concentrations below 0.2 μmol COP35 in lysis buffer (Fig. 3A, middle, arrowhead with band R). We applied nano LC-ESI-Q-TOF MS-MS analysis to identify both "Q" and "R" bands. A search for its tandem mass spectra in the NCBI nr protein database using MASCOT identified these 2 bands, "Q" as the clathrin heavy chain (CHC) with ion score 75 (Fig. 3A, top right), and "R" as GRP78/BiP with ion score 120 (Fig. 3A, bottom right). For further confirmation, RBE cell lysate was precipitated with COP35 or the control peptide (Fig. 3B). The precipitated proteins were subjected to SDS-PAGE (Fig. 3B, left) following immunoblotting analysis with detection using anti-CHC monoclonal antibody (Fig. 3B, middle, arrowhead with CHC) and anti-GRP78 monoclonal antibody (Fig. 3B, right, arrowhead with GRP78). A band of molecular weight of about 190 kDa was recognized by an anti-CHC monoclonal antibody (Fig. 3B, middle, arrowhead with CHC). The CHC band disappeared with a decrease of COP35 titration, whereas no signal was detected in the control peptide precipitation. In addition to the CHC band, a band of around 80 kDa recognized by anti-GRP78 monoclonal antibody appeared (Fig. 3B, right, arrowhead with GRP78). The GRP78 band was most intense at 4.0 μmol concentration in lysis buffer and disappeared at lower COP35 concentration, which was consistent with SDS-PAGE data (Fig. 3A, middle, arrowhead with band R). Next, we confirmed the interaction between CHC and GRP78 by immunoprecipitation (Fig. 3C) and dual immunofluorescence staining of CHC and GRP78 in RBE cells (Fig. 3D). Endogenous GRP78 was found to be coprecipitated with anti-CHC monoclonal antibody (Fig. 3C, αCHC). As controls, the precipitate with anti-GRP78 polyclonal antibody was also detected by anti-GRP78 monoclonal antibody, whereas the precipitate with anti-Myc polyclonal antibody or anti-Flag monoclonal antibody was not detected by anti-GRP78 monoclonal antibody (Fig. 3C). In dual immunofluorescence microscopy, GRP78 clearly colocalized with CHC (Fig. 3D, arrowheads). The green CHC signals were partially merged with GRP78 signals and both appeared to be located in perinuclear cytoplasm and cellular periphery in RBE cells [Fig. 3D, Merge and Merge (high power), arrowheads]. In human resected tumors, we carried out triple immunohistochemical staining for tissues from CCA patients using NHS-fluorescein–labeled COP35 (green), anti-CHC mouse monoclonal antibody with Alexa-Fluor 647–conjugated secondary antibody (blue), and anti-GRP78 rabbit polyclonal antibody with TMR-conjugated secondary antibody (red). We found substantial colocalization between the COP35 and CHC fluorescence signals (blue-green; Fig. 3E, bottom

Published OnlineFirst May 13, 2011; DOI:10.1158/1541-7786.MCR-10-0470

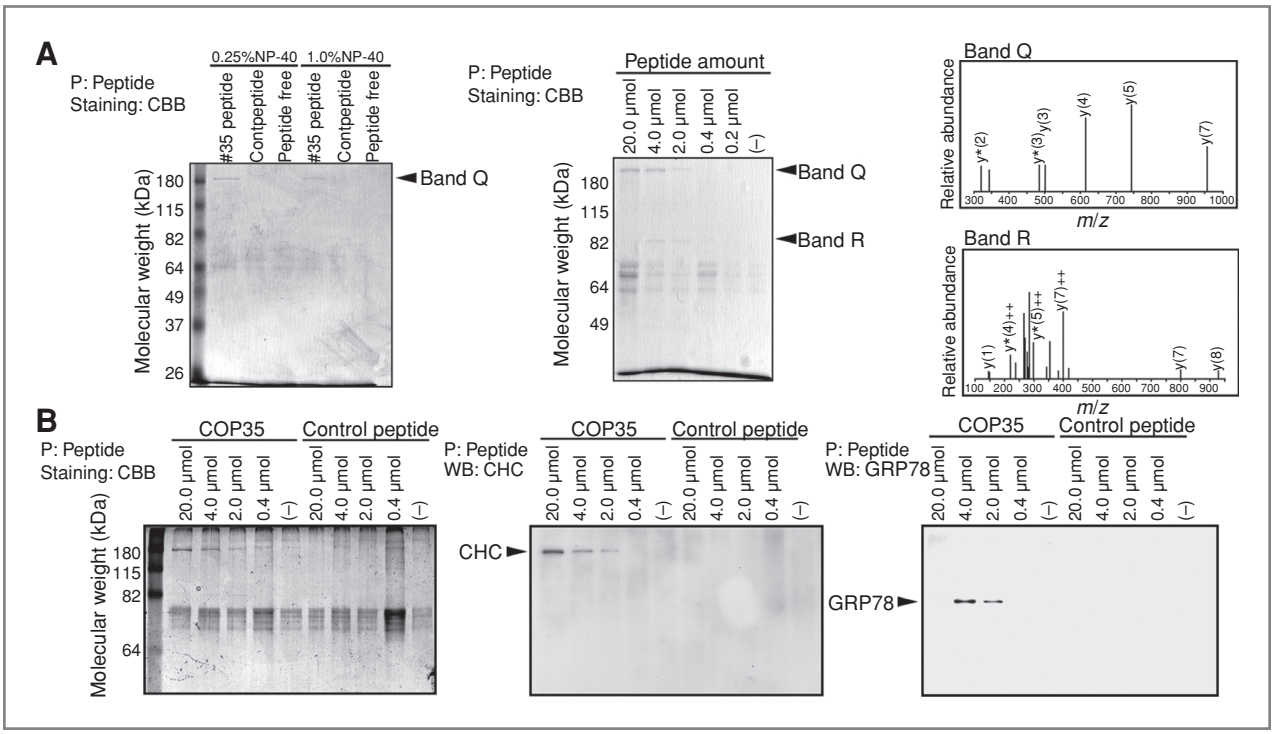

Figure 3. Identification of COP35-binding molecules. A, RBE cells were lysed with different detergent concentrations of 0.25% or 1% NP-40 buffer and precipitated with the biotinylated COP35, the control peptide, or no peptide with streptavidin-conjugated agarose beads. Then, the precipitates were subjected to SDS-PAGE. An approximately 190-kDa band was precipitated with COP35 (left, arrowhead with band Q). RBE cells were lysed with 0.25% NP-40 buffer and precipitated with the titrated concentration of biotinylated COP35 with streptavidin-conjugated agarose beads. Then, the precipitates were subjected to SDS-PAGE. Another approximately 80-kDa band appeared with 4.0 and 2.0 μmol COP35 in lysis buffer (middle, arrowhead with band R). Top and bottom right, spectra of nano LC-ESI-Q-TOF MS-MS analysis of band Q and band R, respectively. B, RBE cells were lysed with 0.25% NP-40 buffer and precipitated with the indicated concentration of biotinylated COP35 or control peptide with streptavidin-conjugated agarose beads. Then, the precipitates were subjected to SDS-PAGE (left) followed by immunoblotting with anti-CHC monoclonal antibody (mAb; middle) and anti-GRP78 mAb (left). P, precipitation; CBB, Coomassie brilliant blue; WB, Western blot.

middle, arrowheads). We also noticed some partial colocalization between COP35 and GRP78 (yellow; Fig. 3E, top right, arrowheads) and these 3 fluorescence signals were merged at the cellular periphery (green-yellow; Fig. 3E, bottom right, arrowheads).

Effect of cellular clathrin depletion on COP35 binding and internalization

To examine whether clathrin-mediated endocytosis is required for COP35-mediated cellular binding and internalization, experiments were carried out in cells depleted of clathrin through treatment with chlorpromazine. RBE cells were incubated with 100 μmol/L NHS-fluorescein–labeled COP35 (Fig. 3F, top, COP35) or a control peptide (Fig. 3F, bottom, control) with or without 5 μg/mL chlorpromazine hydrochloride for 2 hours. As expected, we observed strong intercellular COP35 fluorescence in RBE cells incubated with vehicle saline alone [Fig. 3F, top left, chlorpromazine (−)], whereas the signals were substantially decreased in cells incubated with chlorpromazine hydrochloride [Fig. 3F, top right, chlorpromazine (+)]. No significant fluorescence of control peptide was observed in RBE cells when incubated with either vehicle saline alone or chlorpromazine hydrochloride (Fig. 3F, bottom).

Effect of overexpression, siRNA-mediated silencing of CHC and/or GRP78, or clathrin depletion on 5-FU–mediated tumor inhibition in combination with COP35

To examine whether the enhancement of the 5-FU–mediated tumor inhibitory effect by COP35 depends on CHC and/or GRP78, we evaluated the tumor inhibitory effect of 5-FU with overexpression or siRNA-mediated knockdown of the COP35-binding partners CHC and/or GRP78 in RBE cells (Fig. 4A and B). Furthermore, we evaluated the tumor inhibitory effect of 5-FU in the presence or absence of chlorpromazine (Fig. 4C). We found that the significant difference in tumor inhibitory effect observed between COP35 and control peptide in RBE cells incubated together with 5-FU was enhanced by overexpression of CHC and/or GRP78 (Fig. 4A). Overexpression of CHC and/or GRP78 in transfected RBE cells was confirmed by Western blotting (Fig. 4A, insets). Furthermore, we found a loss of effect of COP35 in enhancing the tumor

Published OnlineFirst May 13, 2011; DOI:10.1158/1541-7786.MCR-10-0470

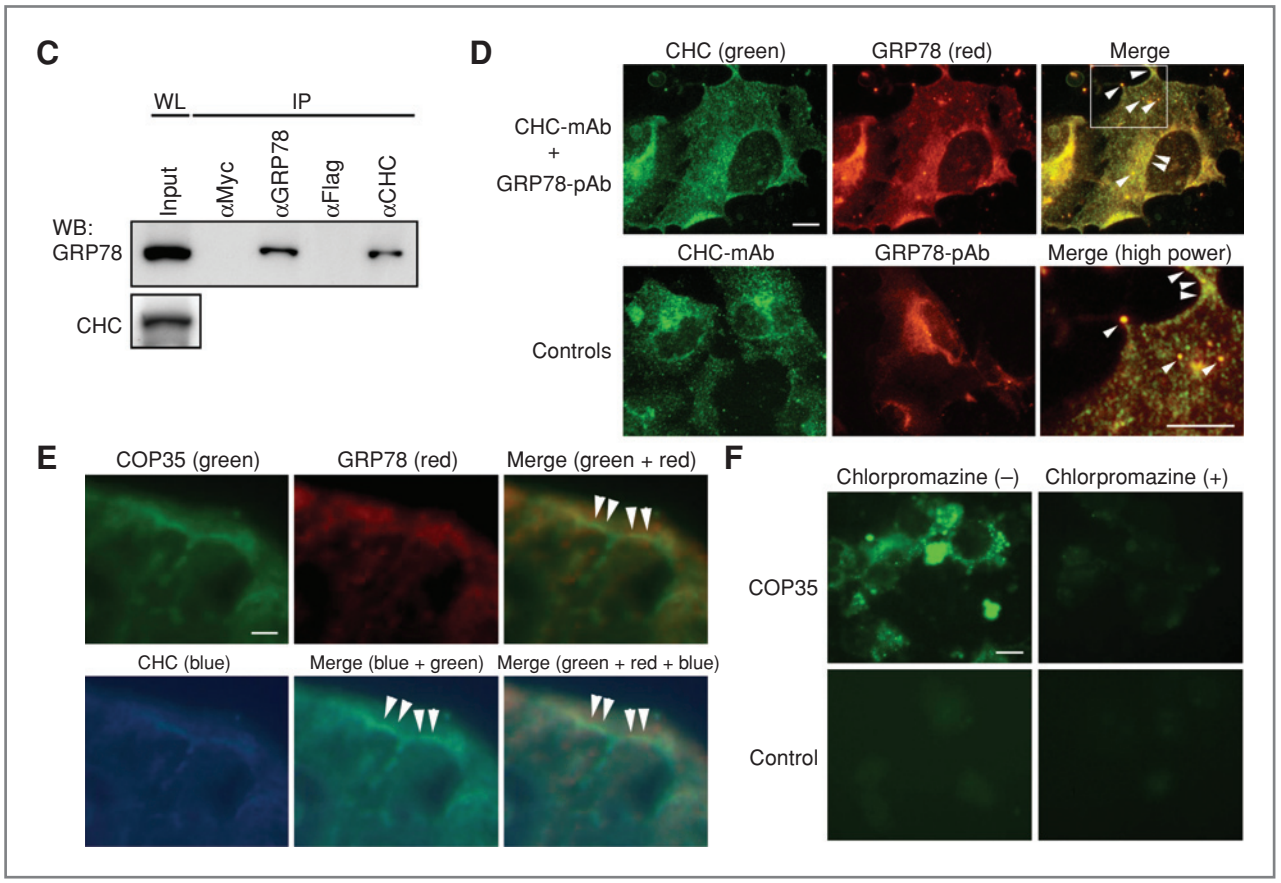

Figure 3. *(Continued)* C, RBE cells were lysed with 0.25% NP-40 buffer and precipitated with anti-Myc polyclonal antibody (pAb; negative control), anti-GRP78 pAb (positive control), anti-Flag mAb (negative control), or anti-CHC mAb. The precipitates were subjected to immunoblotting with anti-GRP78 mAb. D, dual immunofluorescence microscopy of RBE cells. RBE cells were stained with anti-CHC mouse mAb with FITC-conjugated secondary antibody (top left, CHC, green) and anti-GRP78 rabbit pAb with TMR-conjugated secondary antibody (top middle, GRP78, red) and were observed using a fluorescence microscope. Merged images and high-power view of merged images of square field are shown [top right, Merge; bottom right, Merge (high power)]. The yellow merged signals were observed (arrowheads). Single staining controls stained with anti-CHC mouse mAb with FITC-conjugated secondary antibody (bottom left, CHC, green) or anti-GRP78 rabbit pAb with TMR-conjugated secondary antibody (bottom middle, GRP78, red) are shown. Bar is 10 μm. E, triple immunofluorescence microscopy for tissues from CCA patients using NHS-fluorescein–labeled COP35 (top left, COP35, green), anti-CHC mouse mAb with Alexa-Fluor 647–conjugated secondary antibody (bottom left, CHC, blue), and anti-GRP78 rabbit pAb with TMR-conjugated secondary antibody (top middle, GRP78, red). Merged images with yellow, blue-green, and yellow-green are shown [top right, Merge (green + red); bottom middle, Merge (blue + green); and bottom right, Merge (green + red + blue), respectively]. Bar is 10 μm. F, effect of an inhibitor of clathrin-mediated endocytosis, chlorpromazine, on COP35 internalization. RBE cells were incubated with 100 μmol/L NHS-fluorescein–labeled COP35 (top, COP35) or a control peptide (bottom, control), and with [right, chlorpromazine (+)] or without [left, Chlorpromazine (–)] 5 μg/mL chlorpromazine hydrochloride for 2 hours. Bar is 25 μm.

inhibitory effect of 5-FU following the specific knockdown of CHC and/or GRP78 using siRNAs (Fig. 4B). Reduced expression of CHC and/or GRP78 was confirmed by Western blotting (Fig. 4B, insets). Furthermore, we found that the significant difference in tumor inhibitory effects observed between COP35 and control peptide in RBE cells incubated with 5-FU was abolished when RBE cells were incubated with 5 μg/mL chlorpromazine hydrochloride to deplete clathrin (Fig. 4C).

Evaluating the expression of CHC and GRP78 in CCA specimens

We confirmed expression of both CHC and GRP78 by immunohistochemistry in formalin-fixed, paraffin-embedded human CCA specimens (Fig. 5A). We evaluated the immunoreactivity of anti-CHC and anti-GRP78 antibodies in 18 cases [the same patient group as for when we evaluated COP35 binding to clinically resected CCA samples (Table 1)]. Representative figures are shown (Fig. 5A). Evaluations of the immunoreactivity of CHC and GRP78 are presented in Table 1, and plotted in Figure 5B and C. Expression of CHC and GRP78 was found to be higher in ICC [Fig. 5A, ICC (case 1)] and ECC [Fig. 5, ECC (case 16)] than in nontumorous bile duct epithelium [Fig. 5A, normal (case 1)]. Parallel hematoxylin and eosin images are presented (Fig. 5A, bottom). Because there were some normal biliary epithelia in tumor-free tissues in pathologic specimens of cases 1 to 16, we were able to quantify the immunoreactivities of

Published OnlineFirst May 13, 2011; DOI:10.1158/1541-7786.MCR-10-0470

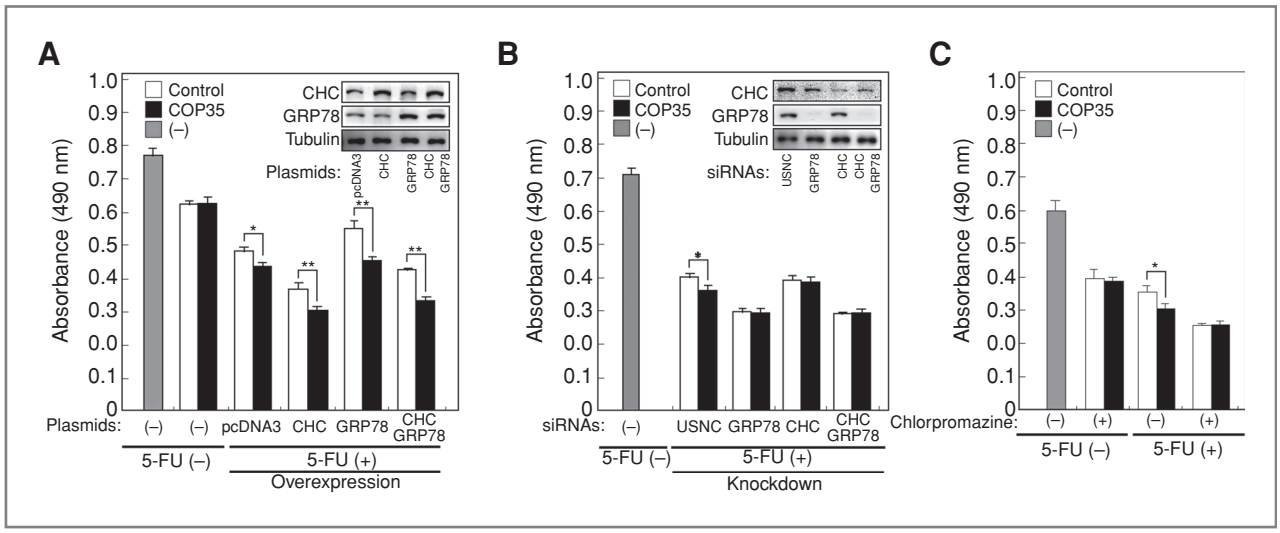

Figure 4. MTS assay to evaluate whether COP35 enhances the tumor inhibitory effect of 5-FU on RBE cells. A, RBE cells transfected with CHC and/or GRP78 expression plasmids or a vector plasmid (pcDNA3) were incubated with 500 μmol/L COP35 or control peptide together with 10 μg/mL 5-FU for 48 hours. B, RBE cells transfected with CHC and/or GRP78 specific knockdown siRNAs or universal scrambled negative control (USNC) siRNA were incubated with 500 μmol/L COP35 or control peptide together with 10 μg/mL 5-FU for 48 hours. Expression levels of CHC and/or GRP78 were confirmed by Western blotting (A and B insets, respectively). C, RBE cells were incubated with 500 μmol/L COP35 or control peptide together with 10 μg/mL 5-FU in the presence or absence of an inhibitor of clathrin-mediated endocytosis, chlorpromazine hydrochloride (5 μg/mL) for 48 hours. Values are the mean and SD results from triplicate cultures. *, $P < 0.05$; **, $P < 0.01$.

CHC and GRP78 in tumor and nontumorous tissues, which were plotted (Fig. 5B and C). We found that the arithmetic mean (M) immunoreactivities of CHC ($M = 2.4$) and GRP78 ($M = 1.3$) in tumor tissues were significantly higher than those of CHC ($M = 1.1$) and GRP78 ($M = 0.062$) in nontumorous tissues with paired t-test probabilities. **, $P < 0.01$ (Fig. 5B and C).

Correlation between COP35 fluorescence intensity and immunoreactivity of CHC and GRP78

Because COP35 bound to both CHC and GRP78, we examined whether COP35 fluorescence intensity positively correlated with the immunoreactivity of CHC and GRP78 in the same patient samples presented in Table 1. We found that COP35 fluorescence intensity was statistically correlated with the immunoreactivity of CHC and GRP78 with Pearson's product–moment correlation coefficient $R = 0.706$ with value of $P = 0.00154$, and $R = 0.531$ with value of $P = 0.0282$, respectively (Fig. 5D and E).

Discussion

CCA is known to have a poor prognosis carcinoma compared with many other malignant tumors (1–4). Novel therapeutics are urgently required to effectively treat CCA. Peptide-presenting phage display libraries are powerful tools for iteratively producing ligands that can bind to specific targets (9–12). In this study, we utilized a phage display library to identify a novel peptide, defined as COP35. COP35 selectively bound to CCA derived from clinically resected specimens from patients as well as CCA cell lines (Figs. 1, 2A and B). Therefore, we consider that COP35 binds to a CCA-specific target ligand. In addition, COP35 was found to enhance the tumor inhibitory effect of 5-FU (Fig. 2C and D).

Using nano LC-ESI-Q-TOF MS-MS, we identified the CHC as a COP35-binding partner (Fig. 3A). The molecular weight of CHC is 192 kDa, which is consistent with our SDS-PAGE results and following immunoblotting detected with anti-CHC monoclonal antibody (Fig. 3A and B). Clathrin is the major protein component of a major class of coated vesicles and plays an important role in endocytosis (24–26), a pathway known to be involved in pathogen internalization (27, 28). We therefore speculated that COP35 is internalized via a clathrin-dependent endocytic pathway by direct or indirect interaction with CHC in living cells. Using TAT peptide as a cell-penetrating positive control peptide for peptide internalization, fluorescence was detected ubiquitously in all cells, whereas fluorescence signal from COP35 was specifically detected in RBE cells and not MMNK-1 cells (Fig. 2A). Thus, it is suggested that the internalization of COP35 in RBE cells may occur in a different way from that for cell-penetrating peptide. Because it was reported that endocytosis might be accelerated in CCA cells because of their motility and high-energy demand (29), we examined the effect of an inhibitor of clathrin-mediated endocytosis, chlorpromazine, to investigate whether COP35 is actually internalized into CCA cells via clathrin-mediated endocytosis. We found that depletion of clathrin using chlorpromazine inhibited the COP35 internalization in RBE

Published OnlineFirst May 13, 2011; DOI:10.1158/1541-7786.MCR-10-0470

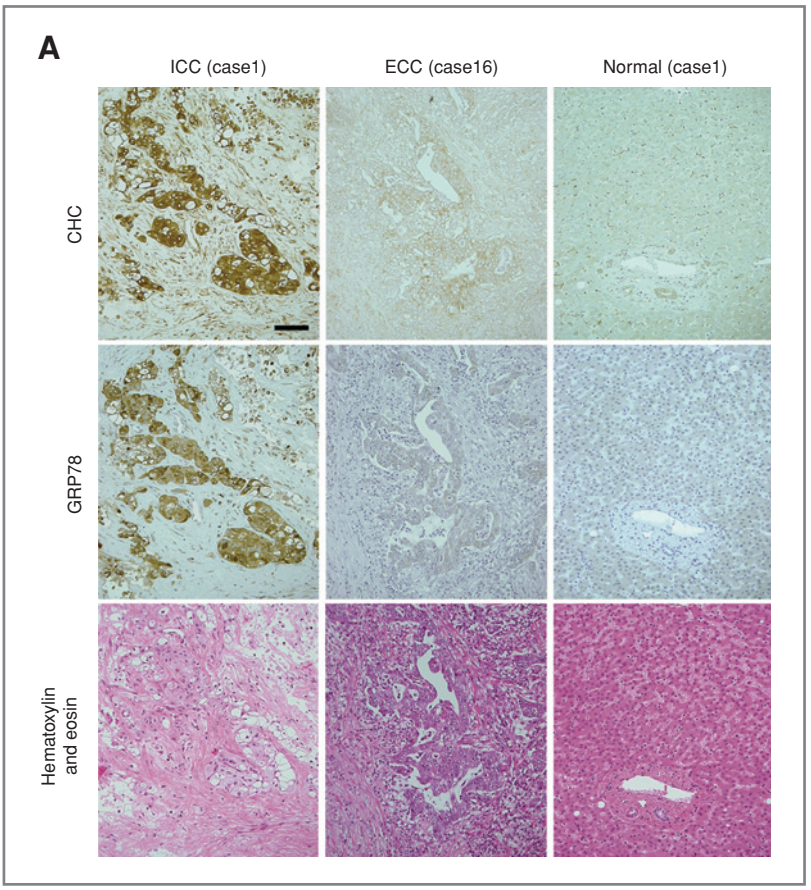

Figure 5. Expression of the CHC and GRP78 in CCA. A, ICC and ECC in formalin-fixed, paraffin-embedded specimens were immunostained with anti-CHC polyclonal antibody (top) or anti-GRP78 polyclonal antibody (middle) or stained with hematoxylin and eosin (bottom). Details are summarized in Table 1. Representative ICC (case 1 in Table 1), ECC (case 16 Table 1), and nontumorous bile duct normal epithelium of CCA (case 1 in Table 1) are presented (normal epithelium). The bar is 100 μm.

cells (Fig. 3F). The result supports our hypothesis that COP35 is internalized via clathrin-mediated endocytosis. It was also suggested that CHC is upregulated in hepatocellular carcinoma tissues (30). Consistent with this, our data suggest that CHC expression in CCA lesions was higher than that in normal bile duct epithelium by immunohistochemical staining of formalin-fixed and paraffin-embedded tissues (Table 1; Fig. 5A, top and B). Thus, it was suggested that CHC could be an attractive target of COP35.

Notably, as we decreased the concentration of COP35, another clear band became apparent around 80 kDa precipitated with CHC (Fig. 3A, middle, arrowhead with band R). The 80-kDa protein was determined to be a glucose-regulated protein of 78 kDa (GRP78, also referred to as BiP; Fig. 3A, right, band R). GRP78 is a member of the HSP70 family that functions as a chaperone critical for folding, maturation, and transport of polypeptides and proteins, which is expressed on the cell surface where it functions as a receptor for a wide variety of ligands (31, 32). GRP78 is also important in the unfolded protein response that ameliorates stress conditions, such as glucose starvation and hypoxia, which are characteristic of malignant tumors, and serves to protect tumor cells against cell death (33, 34). GRP78 has been reported to be strongly expressed in gastric and prostate cancer and correlate with their aggressive behavior and poor prognosis (35, 36). The induction of GRP78 by unfolded protein response during endoplasmic reticulum stress is reported to be required for pathophysiologic conditions such as tumor proliferation, survival, and angiogenesis (37). Consistent with this, our findings indicated that GRP78 was highly expressed in CCA cells (Table 1 and Fig. 5A, middle and C). The interaction between CHC and GRP78 is likely to affect the tumor inhibitory effect of 5-FU. We found that COP35 enhanced the tumor inhibitory effect of 5-FU (Fig. 2C and D), and siRNA-mediated knockdown of CHC and/or GRP78 and chlorpromazine treatment of RBE cells resulted in abolishment of the enhancement of the 5-FU tumor inhibitory effect of COP35 (Fig. 4B and C), whereas overexpression of CHC and/or GRP78 in RBE cells resulted in an enhanced 5-FU–mediated tumor inhibitory effect of COP35 (Fig. 4A). In addition, the ability of COP35 to bind to clinical samples was statistically correlated with the expression of CHC and GRP78 (Fig. 5D and E). Thus, it was suggested that both CHC and GRP78 are important molecules for the function of COP35 in enhancing the tumor inhibitory effect of 5-FU.

As shown in Figure 3, whereas high concentration (20.0 μmol) of COP35 bound only to CHC, the lower concentration (4.0 and 2.0 μmol) of COP35 bound to

Published OnlineFirst May 13, 2011; DOI:10.1158/1541-7786.MCR-10-0470

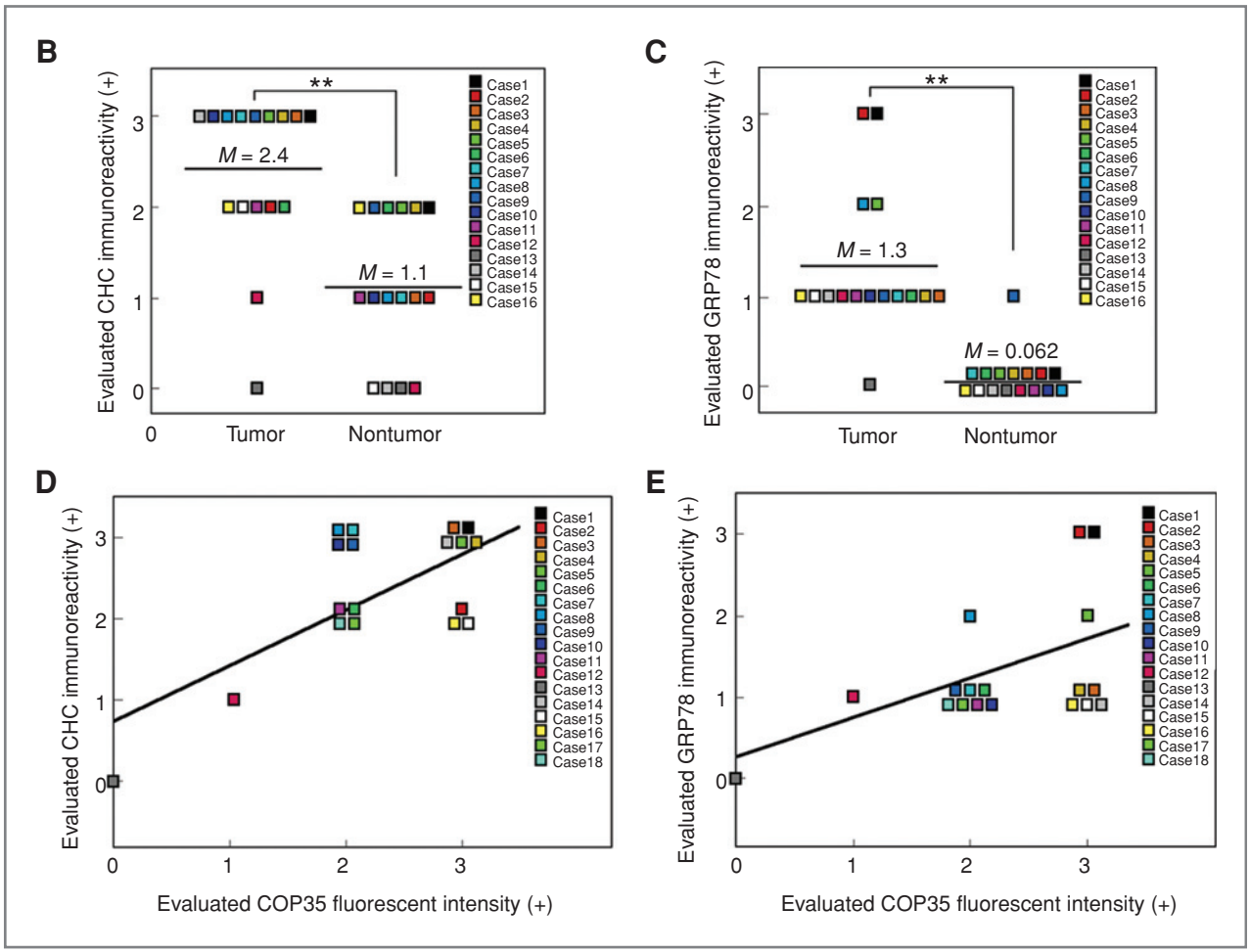

Figure 5. *(Continued)* B and C, differences between immunoreactivity in tumorous tissues and nontumorous tissues. The evaluated immunoreactivities of CHC and GRP78 in tumorous tissues and nontumorous tissues are plotted. The arithmetic means (*M*) of evaluated immunoreactivities of CHC ($M = 2.4$) and GRP78 ($M = 1.3$) in tumor tissues are significantly higher than those of CHC ($M = 1.1$) and GRP78 ($M = 0.062$) in nontumorous tissues with paired *t*-test probabilities. $P < 0.01$. D and E, correlations between COP35 fluorescence intensity and immunoreactivity of CHC and GRP78. Evaluated COP35-fluorescence intensity is on the *x*-axis and evaluated immunoreactivity of CHC or GRP78 is on the *y*-axis. Evaluated COP35 fluorescence intensity is statistically correlated with the evaluated immunoreactivity of CHC and GRP78 with Pearson's product–moment correlation coefficient $R = 0.706$ with a value of $P = 0.00154$, and $R = 0.531$ with value of $P = 0.0282$, respectively.

CHC accompanied by GRP78 (Fig. 3A, middle, and B). We speculate that COP35 could directly bind to CHC, which may interact with a surface receptor protein GRP78. The hypothesis was also confirmed by further evidence that GRP78 was coprecipitated with CHC by immunoprecipitation and appeared to colocalize with CHC by immunofluorescence microscopy (Fig. 3C–E). However, we noted the limitation of our study to explain this finding that COP35 interacts with CHC at high concentration and GRP78 at lower concentration, which may reflect a key function of COP35 on enhancement of the tumor inhibitory effect of 5-FU. We speculated that higher concentration of COP35 might induce a conformational change in CHC that reduces the power of binding between CHC and GRP78 under our experimental conditions.

Additional studies will be required to fully elucidate the mechanism by which COP35 enhances the tumor inhibitory effect of 5-FU prior to clinical studies. It has been reported that a number of prognostic and predictive gene mutations such as *k-ras*, *p53*, and *Raf/Mek/Erk* in tumor can correlate with sensitivity and/or resistance to chemotherapies (38). In patients, germline pharmacogenetic mutations or polymorphisms can influence chemotherapeutic toxicity (38). We speculate that metabolism and degradation by nonspecific peptidases and proteases, or clathrin-dependent endocytosis of macrophages, may be different for each patient. Here, we present data suggesting that tumor expression levels of CHC and GRP78 could be important factors for gauging the likely efficacy of 5-FU in combination therapies of COP35 and 5-FU.

Published OnlineFirst May 13, 2011; DOI:10.1158/1541-7786.MCR-10-0470

Disclosure of Potential Conflicts of Interest

No potential conflicts of interest were disclosed.

Acknowledgments

The authors thank M. Narita, Y. Shimojo, and H. Kawate for their technical assistance.

In Memoriam

Our colleague, a surgeon, F. Maruta, died before publication of this study. This article is dedicated to his memory.

Grant Support

This work was supported by Grants-in-Aid for Scientific Research from the Japan Society for the Promotion of Science (19591581, 20591588) and by grants from the Japan Research Foundation for Clinical Pharmacology and the Public Trust Surgery Research Fund (to S. Miyagawa), and in part by Grants-in-Aid for Research on Measures for Intractable Diseases from The Ministry of Health, Labor, and Welfare, Japan, and a grant from the Hokuto Foundation (to J. Masumoto).

The costs of publication of this article were defrayed in part by the payment of page charges. This article must therefore be hereby marked *advertisement* in accordance with 18 U.S.C. Section 1734 solely to indicate this fact.

Received October 19, 2010; revised May 1, 2011; accepted May 6, 2011; published OnlineFirst May 13, 2011.

References

1. Callea F, Sergi C, Fabbretti G, Brisigotti M, Cozzutto C, Medicina D. Precancerous lesions of the biliary tree. J Surg Oncol Suppl 1993;3:131–3.
2. Khan SA, Thomas HC, Davidson BR, Taylor-Robinson SD. Cholangiocarcinoma. Lancet 2005;366:1303–14.
3. Han JK, Choi BI, Kim AY, An SK, Lee JW, Kim TK, et al. Cholangiocarcinoma: pictorial essay of CT and cholangiographic findings. Radiographics 2002;22:173–87.
4. Sirica AE. Cholangiocarcinoma: molecular targeting strategies for chemoprevention and therapy. Hepatology 2005;41:5–15.
5. Kashentseva EA, Seki T, Curiel DT, Dmitriev IP. Adenovirus targeting to c-erbB-2 oncoprotein by single-chain antibody fused to trimeric form of adenovirus receptor ectodomain. Cancer Res 2002;62:609–16.
6. Fisher KD, Stallwood Y, Green NK, Ulbrich K, Mautner V, Seymour LW. Polymer-coated adenovirus permits efficient retargeting and evades neutralizing antibodies. Gene Ther 2001;8:341–8.
7. Backer MV, Backer JM. Targeting endothelial cells overexpressing VEGFR-2: selective toxicity of Shiga-like toxin-VEGF fusion proteins. Bioconjug Chem 2001;12:1066–73.
8. Barry MA, Dower WJ, Johnston SA. Toward cell-targeting gene therapy vectors: selection of cell-binding peptides from random peptide-presenting phage libraries. Nat Med 1996;2:299–305.
9. Pasqualini R, Ruoslahti E. Organ targeting *in vivo* using phage display peptide libraries. Nature 1996;380:364–66.
10. Maruta F, Parker AL, Fisher KD, Hallissey MT, Ismail T, Rowlands DC, et al. Identification of FGF receptor-binding peptides for cancer gene therapy. Cancer Gene Ther 2002;9:543–52.
11. Akita N, Maruta F, Seymour LW, Kerr DJ, Parker AL, Asai T, et al. Identification of oligopeptides binding to peritoneal tumors of gastric cancer. Cancer Sci 2006;97:1075–81.
12. Shimizu A, Maruta F, Akita N, Miwa S, Seymour LW, Kerr DJ, et al. Identification of an oligopeptide binding to hepatocellular carcinoma. Oncology 2006;71:136–45.
13. Pan W, Arnone M, Kendall M, Grafstrom RH, Seitz SP, Wasserman ZR, et al. Identification of peptide substrates for human MMP-11 (stromelysin-3) using phage display. J Biol Chem 2003;278:27820–7.
14. Aggarwal S, Singh P, Topaloglu O, Isaacs JT, Denmeade SR. A dimeric peptide that binds selectively to prostate-specific membrane antigen and inhibits its enzymatic activity. Cancer Res 2006;66:9171–7.
15. Kelly KA, Jones DA. Isolation of a colon tumor specific binding peptide using phage display selection. Neoplasia 2003;5:437–44.
16. Lee TY, Wu HC, Tseng YL, Lin CT. A novel peptide specifically binding to nasopharyngeal carcinoma for targeted drug delivery. Cancer Res 2004;64:8002–8.
17. Hatakeyama S, Sugihara K, Nakayama J, Akama TO, Wong SM, Kawashima H, et al. Identification of mRNA splicing factors as the endothelial receptor for carbohydrate-dependent lung colonization of cancer cells. Proc Natl Acad Sci U S A 2009;106:3095–100.
18. Arap W, Pasqualini R, Ruoslahti E. Cancer treatment by targeted drug delivery to tumor vasculature in a mouse model. Science 1998;279:377–80.
19. Newton JR, Kelly KA, Mahmood U, Weissleder R, Deutscher SL. *In vivo* selection of phage for the optical imaging of PC-3 human prostate carcinoma in mice. Neoplasia 2006;8:772–80.
20. Maruyama M, Kobayashi N, Westerman KA, Sakaguchi M, Allain JE, Totsugawa T, et al. Establishment of a highly differentiated immortalized human cholangiocyte cell line with SV40T and hTERT. Transplantation 2004;77:446–51.
21. He D, Wilborn TW, Falany JL, Li L, Falany CN. Repression of CFTR activity in human MMNK-1 cholangiocytes induces sulfotransferase 1E1 expression in co-cultured HepG2 hepatocytes. Biochim Biophys Acta 2008;1783:2391–7.
22. Masumoto J, Dowds TA, Schaner P, Chen FF, Ogura Y, Li M, et al. ASC is an activating adaptor for NF-κB and caspase-8-dependent apoptosis. Biochem Biophys Res Commun 2003;303:69–73.
23. Deshayes S, Morris MC, Divita G, Heitz F. Cell-penetrating peptides: tools for intracellular delivery of therapeutics. Cell Mol Life Sci 2005;62:1839–49.
24. Pearse BM. Coated vesicles from pig brain: purification and biochemical characterization. J Mol Biol 1975;97:93–8.
25. Pearse BM. Clathrin: a unique protein associated with intracellular transfer of membrane by coated vesicles. Proc Natl Acad Sci U S A 1976;73:1255–9.
26. Traub LM. Tickets to ride: selecting cargo for clathrin-regulated internalization. Nat Rev Mol Cell Biol 2009;10:583–96.
27. Veiga E, Cossart P. The role of clathrin-dependent endocytosis in bacterial internalization. Trends Cell Biol 2006;16:499–504.
28. Veiga E, Guttman JA, Bonazzi M, Boucrot E, Toledo-Arana A, Lin AE, et al. Invasive and adherent bacterial pathogens co-Opt host clathrin for infection. Cell Host Microbe 2007;2:340–51.
29. Poincloux R, Lizárraga F, Chavrier P. Matrix invasion by tumour cells: a focus on MT1-MMP trafficking to invadopodia. J Cell Sci 2009;122:3015–24.
30. Seimiya M, Tomonaga T, Matsushita K, Sunaga M, Oh-Ishi M, Kodera Y, et al. Identification of novel immunohistochemical tumor markers for primary hepatocellular carcinoma; clathrin heavy chain and formiminotransferase cyclodeaminase. Hepatology 2008;48:519–30.
31. Shiu RP, Pouyssegur J, Pastan I. Glucose depletion accounts for the induction of two transformation-sensitive membrane proteinsin Rous sarcoma virus-transformed chick embryo fibroblasts. Proc Natl Acad Sci U S A 1977;74:3840–4.
32. Gonzalez-Gronow M, Selim MA, Papalas J, Pizzo SV. GRP78: a multifunctional receptor on the cell surface. Antioxid Redox Signal 2009;11:2299–306.

Published OnlineFirst May 13, 2011; DOI:10.1158/1541-7786.MCR-10-0470

33. Gething MJ. Role and regulation of the ER chaperone BiP. Semin Cell Dev Biol 1999;10:465–72.
34. Lee AS. The glucose-regulated proteins: stress induction and clinical applications. Trends Biochem Sci 2001;26:504–10.
35. Zheng HC, Takahashi H, Li XH, Hara T, Masuda S, Guan YF, et al. Overexpression of GRP78 and GRP94 are markers for aggressive behavior and poor prognosis in gastric carcinomas. Hum Pathol 2008;39:1042–9.
36. Daneshmand S, Quek ML, Lin E, Lee C, Cote RJ, Hawes D, et al. Glucose-regulated protein GRP78 is up-regulated in prostate cancer and correlates with recurrence and survival. Hum Pathol 2007;38: 1547–52.
37. Dong D, Ni M, Li J, Xiong S, Ye W, Virrey JJ, et al. Critical role of the stress chaperone GRP78/BiP in tumor proliferation, survival, and tumor angiogenesis in transgene-induced mammary tumor development. Cancer Res 2008;68:498–505.
38. Coate L, Cuffe S, Horgan A, Hung RJ, Christiani D, Liu G, et al. Germline genetic variation, cancer outcome, and pharmacogenetics. J Clin Oncol 2010;28:4029–4037.